

This is an Open Access document downloaded from ORCA, Cardiff University's institutional repository:<https://orca.cardiff.ac.uk/id/eprint/109829/>

This is the author's version of a work that was submitted to / accepted for publication.

Citation for final published version:

McCafferty, Cian, David, Francois, Venzi, Marcello, Lorincz, Magor L., Delicata, Francis, Atherton, Zoe, Recchia, Gregorio, Urban, Gergely, Lambert, Regis C., Di Giovanni, Giuseppe, Leresche, Nathalie and Crunelli, Vincenzo 2018. Cortical drive and thalamic feed-forward inhibition control thalamic output synchrony during absence seizures. *Nature Neuroscience* 21 , pp. 744-756. 10.1038/s41593-018-0130-4

Publishers page: <http://dx.doi.org/10.1038/s41593-018-0130-4>

Please note:

Changes made as a result of publishing processes such as copy-editing, formatting and page numbers may not be reflected in this version. For the definitive version of this publication, please refer to the published source. You are advised to consult the publisher's version if you wish to cite this paper.

This version is being made available in accordance with publisher policies. See <http://orca.cf.ac.uk/policies.html> for usage policies. Copyright and moral rights for publications made available in ORCA are retained by the copyright holders.



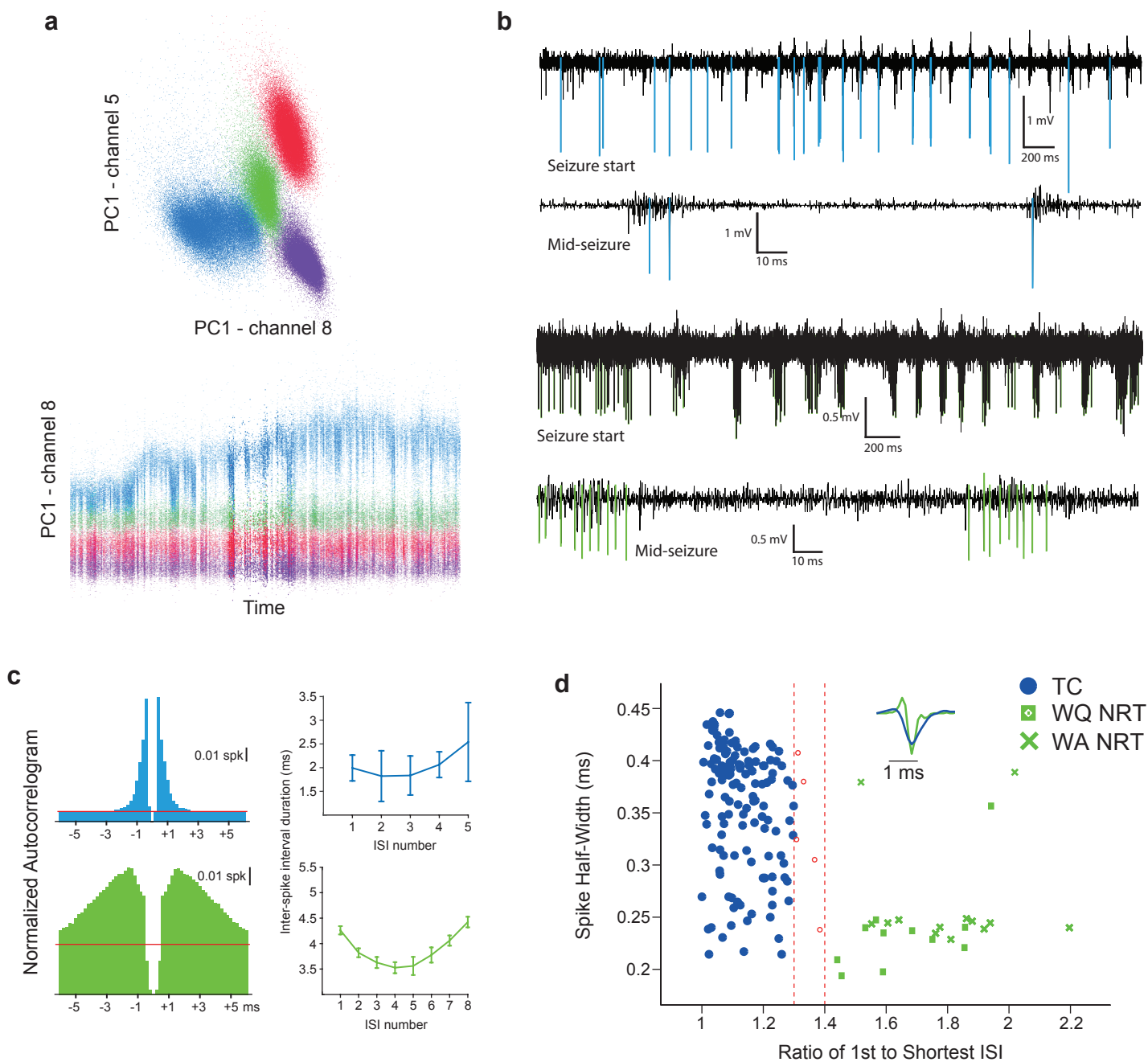


Figure 1

Figure 1. Spike clustering and thalamic neuronal type identification.

(a) Automated spike sorting by clustering of principal components (PC) in multiple dimensions, reflecting spike amplitude and spike shape. (b) High-pass filtered traces showing typical isolated action potentials of TC (blue, top two traces) and NRT (green, bottom two traces) neurons spikes at start and middle of ASs. (c) Autocorrelograms (left) and plots of interspike interval (ISI) versus interspike number of high frequency bursts (right) for a TC (blue) and a NRT neuron (green) during ASs. Note the clear NRT neuron accelerando-decelerando pattern. (d) Spike half-width vs. burst acceleration index (ratio of 1st to shortest ISI in a burst) for all neurons. Red dashed lines indicate acceleration index <1.3 for TC and >1.4 for NRT neurons used to identify the two neuron types (Online Methods). Neurons marked in red were excluded from further analysis. Inset depicts superimposed typical TC (blue) and NRT (green) spike waveforms.

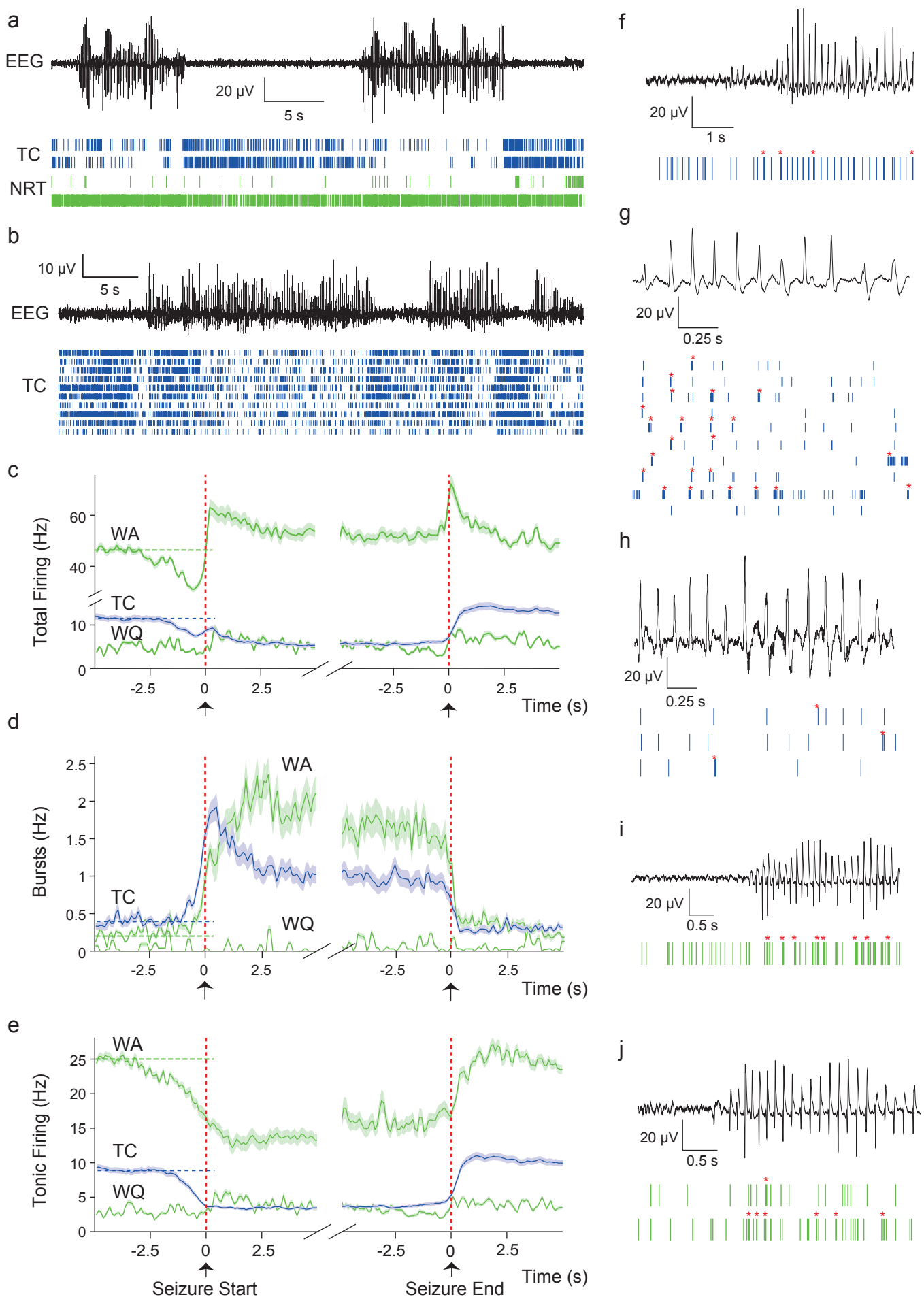


Figure 2

Figure 2. Temporal dynamics of TC and NRT neuron ensemble firing during ASs in GAERS.

(a) Spike-time raster plots (bottom traces) from 2 TC (blue) and 2 NRT (green, top wake-quiescent, bottom wake-active) neurons with time-matched EEG (top trace) in a GAERS. Note the sparse firing of TC neurons during ASs and the diverse firing of the two NRT neurons. (b) Spike-time raster plots (bottom traces) from 10 TC neurons with time-matched EEG (top trace) in another GAERS. Note the decrease in TC neuron firing during ASs. (c,d,e) Temporal evolution of total (c), burst (d) and tonic (e) firing before, during and after ASs for TC (blue) and NRT neurons (green) (lines: mean, shaded areas: \pm SEM) (n=1216 SWDs; n=127 TC neurons; n=11 wake-active, WA, and 8 wake-quiescent, WQ, NRT neurons). Note the similar rate of increase (1.2 Hz/s) of bursts in TC and NRT neurons from about 1 s before SWD detection in the EEG. At the time of the peak of burst firing of TC neurons, NRT bursts continue to increase but at a slower rate (0.5 Hz/s). Vertical red dashed lines indicate the start and end of SWDs in the EEG; horizontal dashed lines indicate mean pre-ictal firing rates. (f-j) Spike-time raster plots (bottom traces) and time-matched EEG (top trace) for different TC and NRT neurons at interictal-to-ictal transitions (f,i,j), at the very start of an AS (g) and in the middle of an AS (h). Note the high prevalence of bursts (red asterisks) in TC and NRT neurons at the start of ASs.

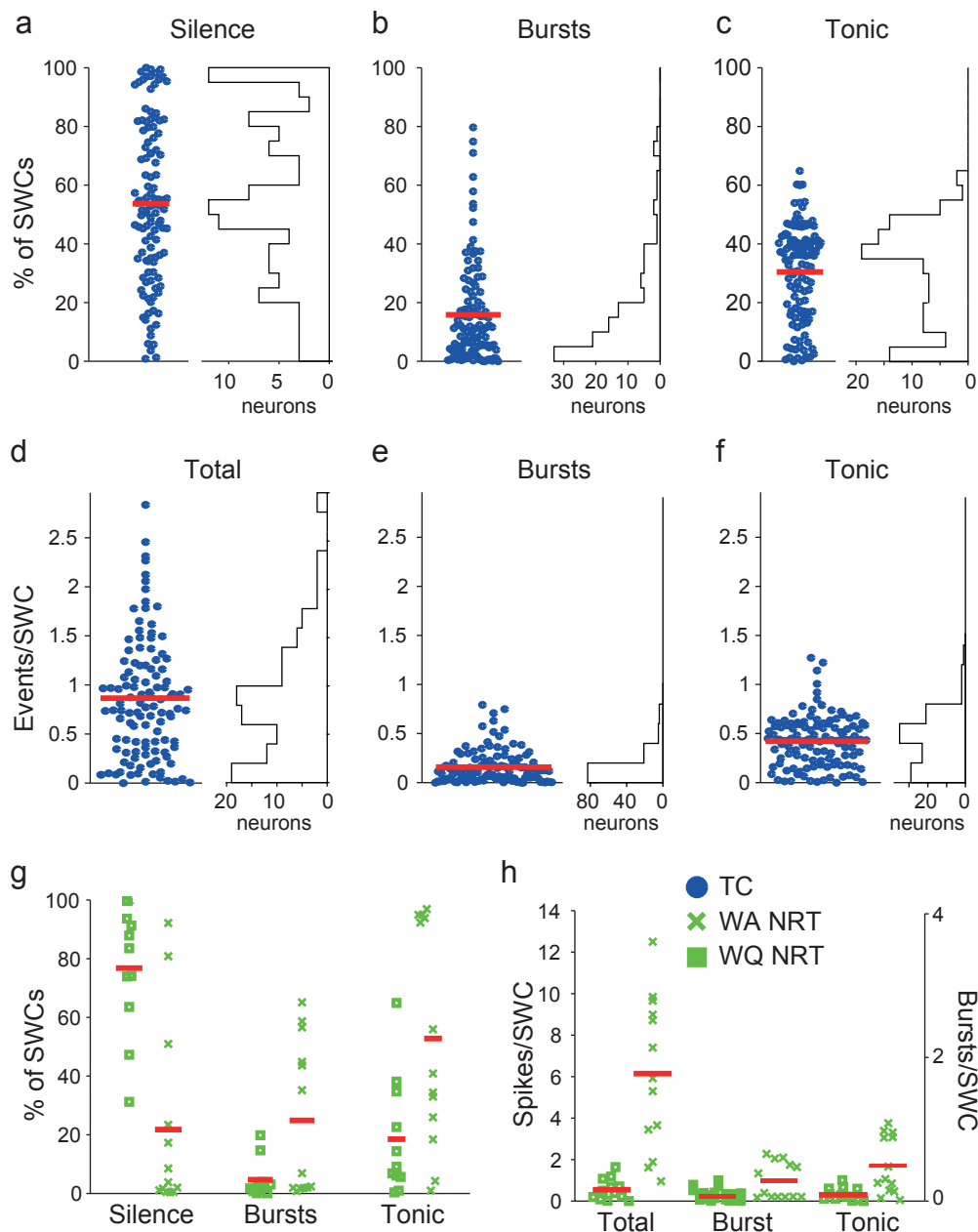


Figure 3

Figure 3. Ictal firing properties during ASs in GAERS.

(**a,b,c**) Electrical silence (**a**), and bursts (**b**) and tonic (**c**) firing observed at each SWCs are plotted as percentage of SWCs for each TC neuron (left) and as distribution for the TC neuron population (right) (n=125). Twelve (9%) TC neurons were completely silent during ASs and 62 (45%) were silent for >50% of SWCs. Moreover, 33 (24%) TC neurons showed no burst during ASs, 84 (61%) neurons exhibited bursts for <20% of SWCs and no TC neuron had bursts for >80% of SWCs. (**d,e,f**) Number of events per SWC for total (**d**), bursts (**e**) and tonic firing (**f**) are plotted for each TC neuron (left) and as a distributions for the TC neuron population (right) (n=125). (**g**) Same plots as in **a-c** for WA and WQ NRT neurons. (**h**) Same plots as in **d-e** for WA and WQ NRT neurons. Red lines in **a-h** indicate mean values.

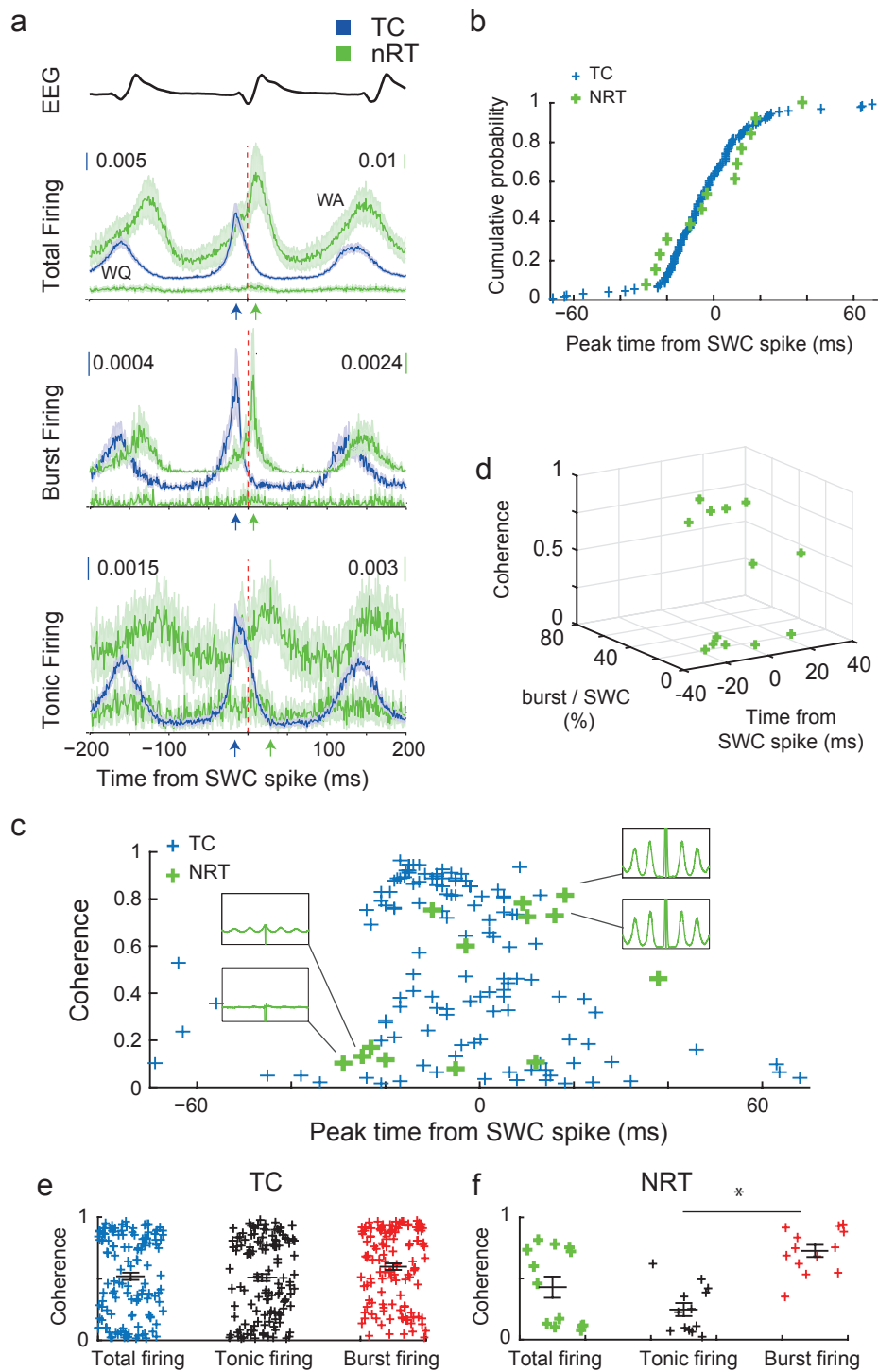
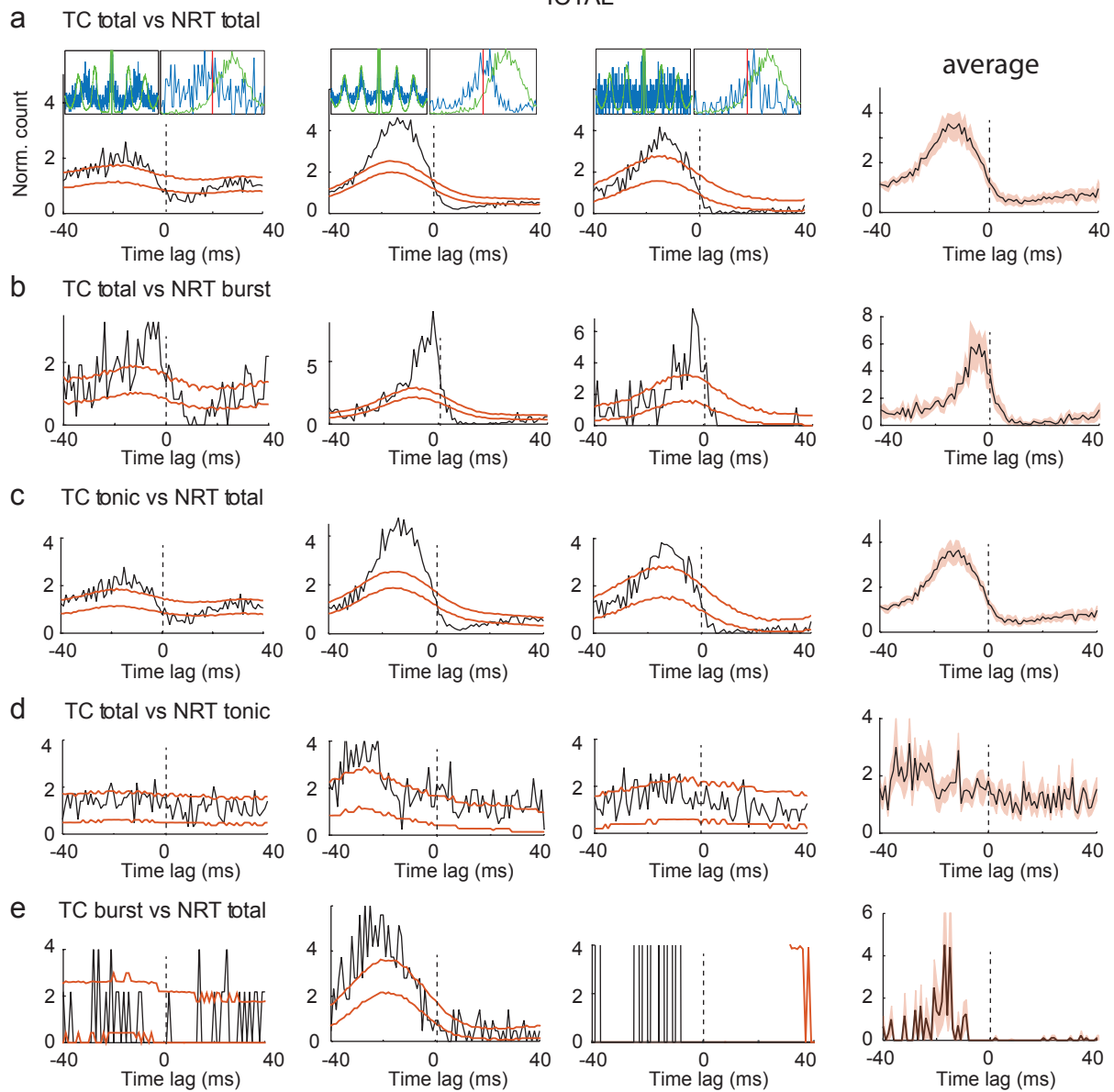


Figure 4

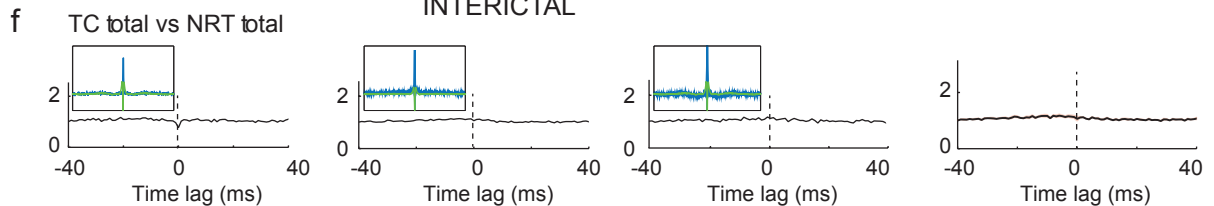
Figure 4. Synchrony and coherence of TC and NRT neuron firing during ASs.

(a) SWC-spike-triggered averages (lines: mean; shaded areas: \pm SEM) of total, burst and tonic firing for GAERS TC (n=139), WA (n=13) and WQ (n=12) NRT neurons. Note the different peak time (color-coded arrows) of TC and NRT neurons relative to SWC spike (red vertical line). (b) Cumulative probability distributions of peak time of total firing for individual TC (blue) and WA NRT (green) neurons show no statistical difference between the two neuronal populations ($p=0.631$; Kolmogorov-Smirnov test). (c) SWC coherence of total firing vs peak time of total firing for individual GAERS TC and WA NRT neurons. Note the high coherence for TC neurons with peak firing times between -20 to 0 ms. In contrast, NRT neurons show low coherence (and flat autocorrelograms, left green insets) when their firing peaks occur in the -20 to 0 ms interval but high coherence (and clear peaks in the autocorrelograms, right green insets) when their firing peaks is after 0 ms. (d) 3D-plot showing NRT neurons with high coherence have a relatively high burst rate and fire relatively late with respect to the SWC-spike, while those NRT neurons with low coherence have a relatively low burst rate and fire early with respect to the SWC spike. (e) SWC coherence for different firing types (mean \pm SEM in black) for individual TC (e) and NRT (f) neurons. Note the higher coherence of burst vs tonic firing in NRT neurons (* $p<0.001$).

ICTAL



INTERICTAL



SLEEP

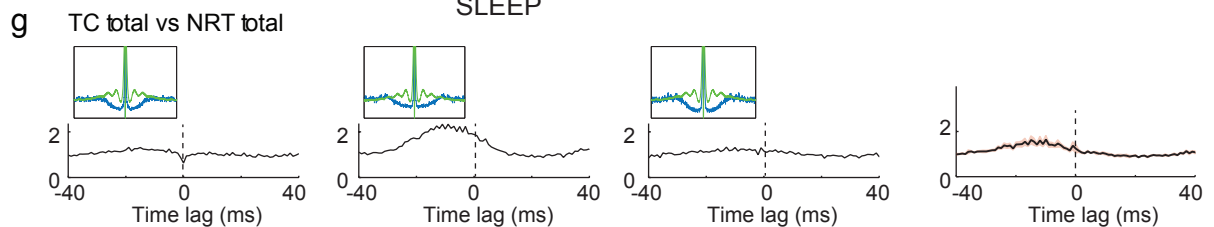


Figure 5

Figure 5: Ictal recruitment of NRT-TC neuron inhibitory assemblies.

(a-g) Representative crosscorrelograms (XCors) (black trace) of firing of three representative pairs of simultaneously recorded TC and NRT neurons (3 leftmost columns) (orange lines indicate expected confidence intervals (5-95%) estimated from surrogate firing time trains for each neuron in its respective firing distribution relative to the SWC) (Supplementary Methods). The average XCors (black line; red shadow: \pm SEM) of 5 pairs is shown in the rightmost column. The significant (below CI) troughs after 0 ms in the XCors indicates a lower probability of the TC neuron to fire after an NRT spike (a), and is maintained when NRT burst firing (b) or TC tonic firing (c) are used for the analysis. No statistically significant sharp peak or trough is present when NRT tonic firing (d) or TC burst firing (e) are used. The same 3 pairs do not exhibit these peaks or troughs during interictal periods (f) and non-REM sleep (g). Top left insets in (a,f,g) show superimposed autocorrelograms for the respective TC (blue) and NRT (green) neurons calculated between -400 and +400 ms from the SWC-spike. Top right insets in (a) show superimposed spike distribution of the respective TC (blue) and NRT (green) neuron calculated from -40 to +40 ms of the SWC-spike (red lines).

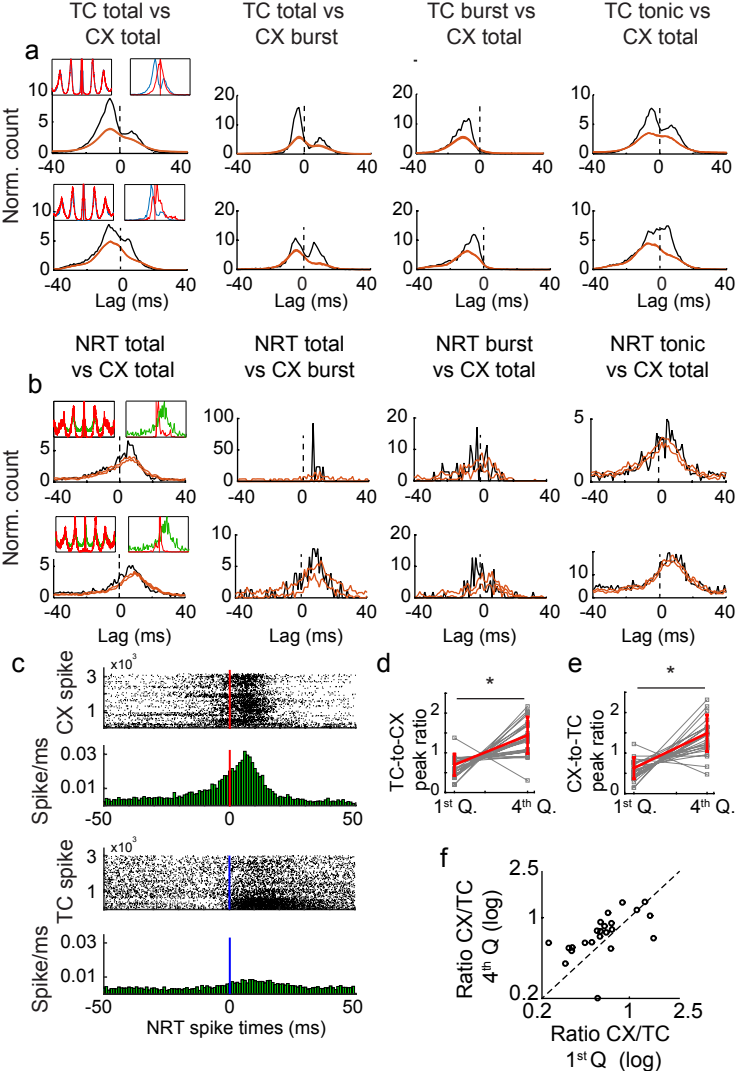


Figure 6

Figure 6: Ictal cortical drive of thalamic neuronal populations.

(a) Representative crosscorrelograms (XCors) (black trace) of firing of two representative pairs of simultaneously recorded TC and cortical (CX) neurons (orange lines indicate expected confidence intervals (5-95%) estimated as described in Fig. 5). The presence of two peaks, one before and one after time-zero, which are more evident when only CX neuron bursts were used for the analysis, indicates reciprocal excitation between TC and CX neurons. (b) Representative XCors as in (a) but for two representative pairs of simultaneously recorded NRT and CX neurons. The significant peak after time zero indicates the increased probability of NRT neuron firing following CX firing. Note how this peak is much larger and sharper when only CX burst firing is used for the analysis. Top left insets in (a) show superimposed autocorrelograms for the respective TC (blue) and CX (red) neurons calculated between -400 and +400 ms from the SWC spike. Top right insets in (a) show superimposed spike distribution of the respective TC (blue) and CX (red) neuron calculated from -40 to +40 ms with respect to the SWC-spike (red lines). Top left and right insets in (b) are as in (a) but for NRT (green) and CX (red) neurons. (c) Peri-spike raster plots (top graphs) and histograms (bottom graphs) of NRT firing with respect to CX and TC neuron firing occurring at time 0 (green lines), calculated from simultaneously recorded CX-NRT and TC-NRT pairs. In the histograms, note the clear peak (6th bin after time-zero) following CX but not TC neuron firing (horizontal red and blue line, respectively). (d) Ratio of the Xcors peak of TC-to-CX interaction (i.e. peak before time-zero) for the 1st and 4th quartiles of SWC-spike amplitudes over peaks for all SWC-spike amplitudes (Supplementary Figure 10b) (Supplementary Methods) ($p=1.26e^{-4}$, signed rank test, $n=25$ pairs). (e) Same plot as (d) for the XCors peak of CX-to-TC interactions (i.e. peak after time-zero) ($p=3.04e^{-5}$, $n=25$ pairs). (f) Ratio of CX-TC and TC-CX peaks for the highest versus the lowest SWC-spike amplitude quartile indicate a gain of cortico-thalamic over the thalamo-cortical contribution to the XCors ($p=5.3e^{-3}$, $n=25$) for the largest SWC-spike.

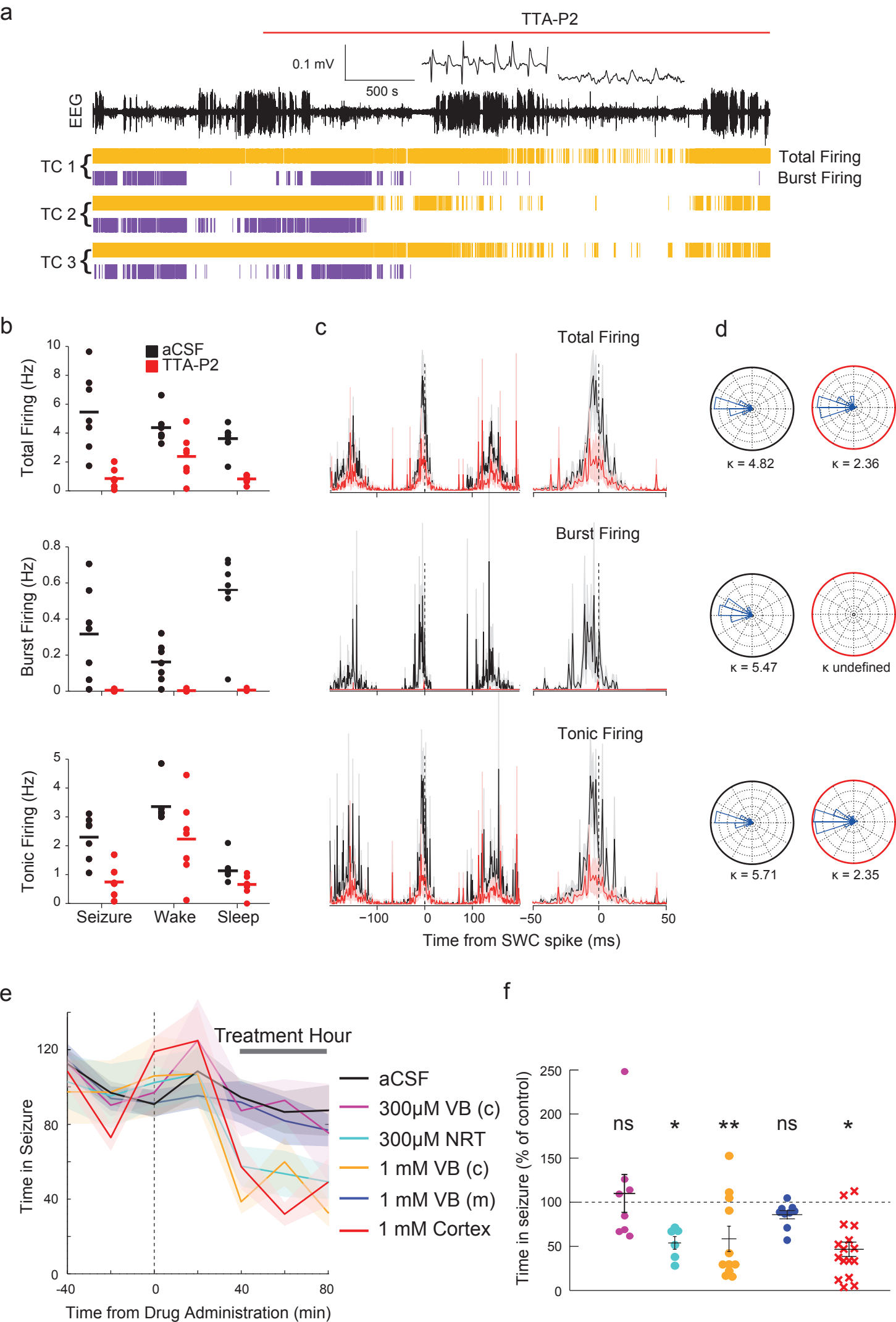


Figure 7

Figure 7. Block of T-channels in NRT and S1pO cortex markedly reduces ASs whereas block in TC neurons does not affect thalamic output synchrony or behavioural ASs.

(a) EEG (top trace), and spike-time (yellow) and burst-time (violet) raster plots (bottom traces) from 3 simultaneously recorded TC neurons in GAERS VB before and during reverse microdialysis administration of 300 μ M TTA-P2 (marked by red line) from an adjacent microdialysis probe. Note the complete block of bursts by TTA-P2 during both ASs and sleep periods (enlarged left and right trace, respectively, at the top of the EEG record). (b) Rates of different firing types before (black) and during (red) complete block of bursts by TTA-P2 show decrease in total ($p < 0.01$), burst ($p < 0.001$), and tonic ($p < 0.05$) firing during ASs, and in total ($p < 0.05$) and burst ($p < 0.01$) but not tonic ($p > 0.05$) firing during wakefulness. Each point represents the average firing of 7 TC neurons (lines are the mean). (c) SWC-triggered averages of different firing types (total, burst, tonic) of 7 TC neurons show clear peaks near the EEG SWC spike (indicated by the vertical black dashed line) before (black) and during (red) complete block of bursts by TTA-P2. (d) Circular firing distribution and circular concentration coefficient (κ) showing similar value before (black circles) and during TTA-P2 (red circles) administration ($n = 7$, Kuiper test, $p > 0.05$; κ undefined for burst firing during TTA-P2 dialysis since bursts were completely abolished). (e) Time-course of total time in seizure before and during bilateral thalamic reverse microdialysis of aCSF or different concentrations of TTA-P2 in GAERS (lines and shaded areas: mean \pm SEM; Treatment Hour indicates the period analysed in f). Black dashed vertical line indicates the start of TTA-P2 dialysis. $n = 8$ GAERS with 300 μ M TTA-P2 in the centre of the VB (VB(c)), 11 with 1mM TTA-P2 in VB(c), 6 with 300 μ M in NRT, 9 with TTA-P2 medially to the centre of the VB (VB(m)) and 16 with 1 mM TTA-P2 in S1pO cortex. Note that microdialysis of 1mM TTA-P2 in VB(c) blocks bursts both in VB and NRT⁴³. (f) Total time spent in seizure by GAERS during different TTA-P2 applications was calculated during the treatment hour as percentage of the control hour (prior to TTA-P2 administration) (color-code as in e; black horizontal lines: mean (\pm SEM), * $p < 0.05$, ** $p < 0.01$, ns: $p > 0.05$). The effect of TTA-P2 on number and duration of ASs, and on SWD frequency is illustrated in Supplementary Fig. 12.

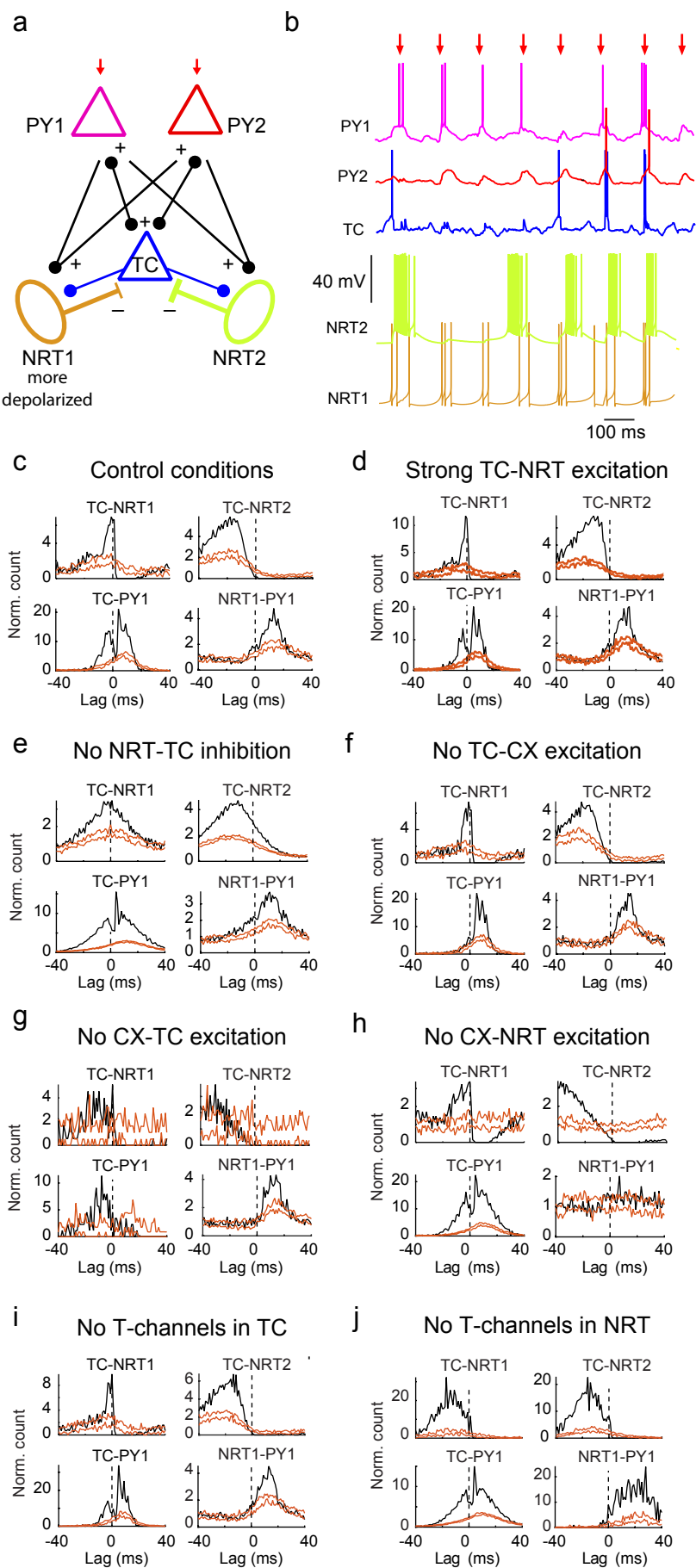


Figure 8

Figure 8. Firing interactions in a cortico-thalamic network model.

(a) Schematic diagram of the model network, consisting of 1 TC, 2 NRT and 2 excitatory cortical pyramidal neurons (PY). NRT1 is more depolarized than NRT2 via steady injected current. Excitatory (AMPA) synapses connect TC to NRT and PY neurons, and PY neurons to NRT and TC neurons. Inhibitory GABA_A synapses connect NRT to TC neurons. Only PY neurons receive a train of 5 AMPA EPSPs that is repeated at a frequency of 7 Hz (red arrows indicate the 3rd EPSP in the train which was used as time-reference for the analysis). (b) Example membrane potential traces illustrate the firing dynamics during 7 Hz stimulation protocol. Note the presence of high frequency bursts in NRT2 and their paucity in TC and NRT1 neuron. (c-j) XCors (black) of simulated firing of different neuron pairs under various conditions (orange lines indicate expected confidence intervals (5-95%) estimated as in Fig. 5 using the 3rd EPSPs as time-reference). The simulation under “control” conditions well reproduced the experimental XCors (c), and no major change was observed in simulations with an increase in the strength of the TC-to-NRT neuron synapse up to 6-fold that of the CX-NRT neuron synapses (d), whereas blocking the NRT-to-TC neuron GABA_A synapses abolished the trough after time zero in TC-NRT neuron XCors (e). Block of cortical to TC neuron synapses or vice versa led to TC-CX XCors that were different from those observed experimentally (f, g), and while a trough was still present in TC-NRT XCors when the cortical input to NRT neurons was absent, there was no peak in NRT-CX XCors (h). Removal of T-channels in TC neurons had no major effect on the XCors (i), whereas in NRT neurons led to broader XCors peaks (j) compared to the control conditions (a).